Optica Applicata, Vol. XXXIII, No. 4, 2003

Thermal characterization of micro-devices with far and near field microscopy

ROMAN F. SZELOCH[1], TEODOR P. GOTSZALK[1], PAWEŁ JANUS[2]

[1]Faculty of Microsystem Electronics and Photonics, Wrocław University of Technology, Wybrzeże Wyspiańskiego 27, 50–370 Wrocław, Poland, e-mail: rszel@wemif.pwr.wroc.pl.

[2]Institute of Electron Technology, al. Lotników 32/46, 02–668 Warszawa, Poland.

After a brief survey of several applications of scanning thermal microscopy (SThM) developed for high resolution thermal diagnostics we present results of thermal analysis of two types of MEMS. Firstly, we have applied our far field thermographic system for analysis of thermal behaviour of the silicon cantilever fabricated as a sensor for a femtocalorimeter near field system. The next results are linked with application of SThM system with the Wollaston probe in micro-thermal measurements of atomic force microscopy (AFM) cantilever.

Keywords: scanning thermal microscopy, thermal characterization, AFM.

1. Introduction

During the past 20 years rapid progress in microelectronic technology has been observed. The result of this process is the development of new measurement techniques that are needed to test the manufactured devices and materials. Modern technology of electronic components, sensors and micro-electro-mechanical system (MEMS) is increasingly concerned with the control of materials at the sub-micrometer down to nanometer scale. In most experiments micro- and nanometer resolution of the investigations is required. Additionally phonon head conduction mechanism in micro- and nanostructures may differ significantly from that in macro-structures. CHEN *et al.* [1], [2] concluded that the phonon size effect includes: increased phonon scattering at the boundaries and interfaces, phonon rarefaction surrounding small structures, and the modification of the phonon dispersion relations. JOSHI and MAJUMDAR [3] have shown that ballistic and diffusive phonon transport is linked with thermal effect under small time and spatial scales. On the other hand, size reduction increases the rate of head generation which leads to a high thermal load on the micro-device. Studying the thermal behaviour of micro- and nanoobjects is essential for predicting the performance of microelectronics and microsystem devices.

Scanning probe microscopy (SPM) is a relatively new tool in characterisation of MEMS electronic materials and components. The progress of this technique was stimulated by the invention of the scanning tunnelling microscope (STM) by BINNIG and ROHRER in 1981 [4]. In recent years, a number of new types of SPM have been developed. SThM was used by HAMMICHE *et al.* [5] to achieve sub-surface imaging of metallic particles embedded in a polymer matrix, using a probe which can act as both ohmic heater and thermometer. Thermal exchange between a probe and a sample in SThM system with Pt resistance wire used in mode of an AFM was investigated by GOMES *et al.* [6]. Application of SThM for comparison of thermal conductivities of CVD-diamond samples is presented by ALTES *et al.* [7]. The effect of dislocations on thermal coductivity in wurtzite GaN layers was investigated by KOTCHETKOV *et al.* [8]. Theoretical predictions are in good agreement with experimental data obtained from SThM. MILLS *et al.* [9] concluded that sub-surface void thermal imaging of VLSI devices using SThM is a practical technique. SZELOCH *et al.* [10] report on applications of SThM for detections of irregularities and soft error in the MEMS body.

2. Thermal properties of the piezoresistive cantilever – femtocalorimeter

Scanning probe microscopy is a very versatile instrument enabling precise surface investigations. The sensitivity of the SPM depends on the parameters of the detector system, which is used to observe the cantilever motions. In our experiments, we have observed a cantilever (femtocalorimeter) with integrated Wheatstone piezoresistive bridge as a deflection sensor [11]–[17]. In this paper, we will analyse thermal behaviour of the cantilever, Figs. 1 and 2. The silicon beam of the femtocalorimeter is coated with SiO_2 layer. Because the thermal expansion coefficient of that material

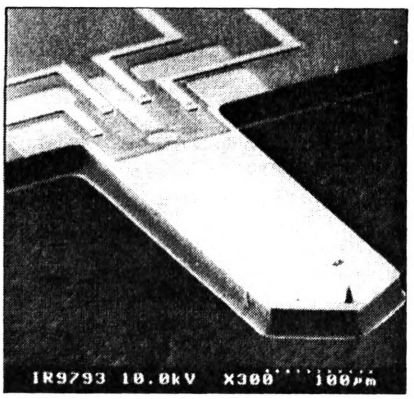

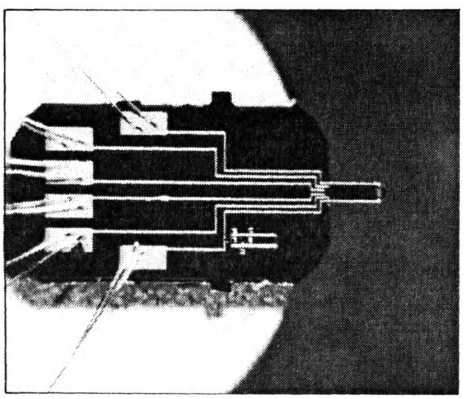

▲

Fig. 1. Single cantilever with integrated sensor and silicon tip [2].

Fig. 2. Piezoresistive femtocalorimeter mounted on the piezoactuator.

differs from the thermal expansion coefficient of the silicon body the designed and manufactured device is sensitive to temperature variations.

In thermal experiments, we have applied our far field infrared microscope with, cooled in LN_2 HgCdMnTe, IR detector (measurement bandwidth from 1 up to 13 μm) [18], [19]. The precise *XY* stepper motor stage was applied to scan the sample under the IR detector (scan resolution – 5 μm). The temperature of the sample stage was controlled with the accuracy of 0.1 °C using Peltier cooler controlled by home built electronics.

We investigated measurement properties of the piezoresistive beam at various temperatures. The resonance curves of the piezoresistive cantilever, observed in the temperature range from 18.2 °C up to 40 °C, are shown in Fig. 3. The IR far field microscope was applied to determine the IR radiation from the Al metalization wires at various device temperatures (Fig. 4). Using this curve we calibrated the images of the IR radiation emitted on the cantilever surface. Figure 5 shows the SEM picture of the structure under investigation and Fig. 6 presents the image of the IR radiation when

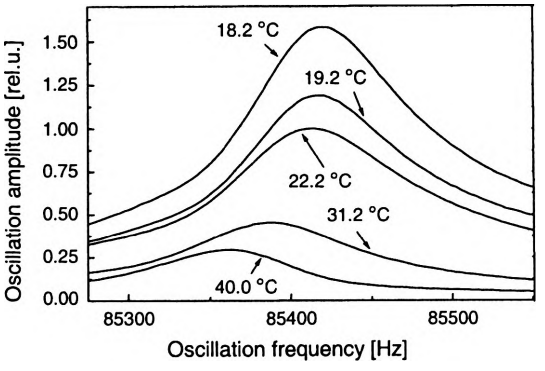

Fig. 3. Resonance curve of the piezoresistive calorimeter observed at various temperatures.

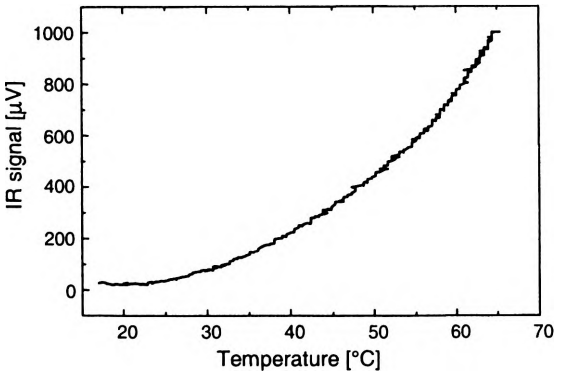

Fig. 4. IR radiation emitted on the Al microheater *vs.* temperature.

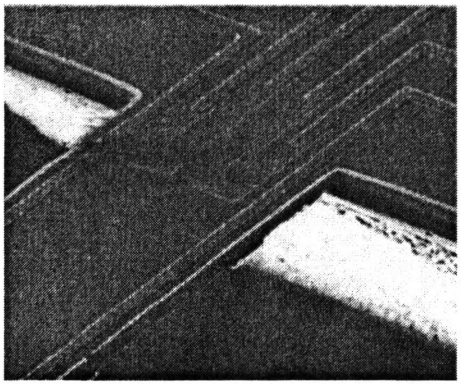

Fig. 5. SEM image of the piezoresistive sensor (picture size 500×500 μm).

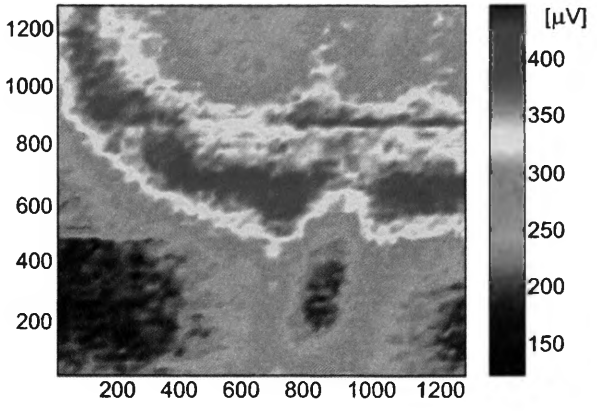

Fig. 6. IR image of the Al line (temperature of the structure 50 °C, scanfield 1200×1200 μm).

the piezoresistive detector is supplied with voltage of 3 V. According to the curve shown in Fig. 4 the temperature of the beam supporting part is estimated in the range of 50 °C.

The results obtained suggest that the designed IR far field thermography system can be applied in investigation of thermal properties of electronic devices with the local resolution of 5 μm and temperature accuracy of 0.2 K.

3. Scanning thermal microscopy

Scanning thermal microscopy is a method with evolved from SPM in the mid-1990s [8]. In the first experiments thermal imaging was carried out using the same silicon cantilever as usually applied in AFM. In these experiments thermal effect on the geometrical topography was linked with changes of input thermal power in the sample [9]. In the next years, several types of the thermal probes appeared, for instance,

thermoelectric couple thermo-sensitive resistor as a sensor, micromechanical calorimeter with piezoresistive deflection sensors.

Thermal probe used in our SThM is capable of performing three functions: it exerts a force on the sample surface (AFM), it acts as a highly localised heat source, either constant or modulated, and it measures heat flow.

In our near-field option (SThM) conventional AFM cantilever is replaced with a miniature thermal probe. This probe consists of V-shaped resistive thermal sensor integrated at the end of a cantilever [20]. The resistive sensor is a platinum/rhodium wire bent to a thermal probe (Fig. 7).

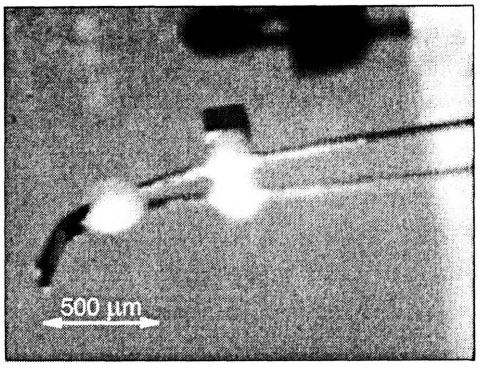

Fig. 7. Scanning thermal microscopy probe.

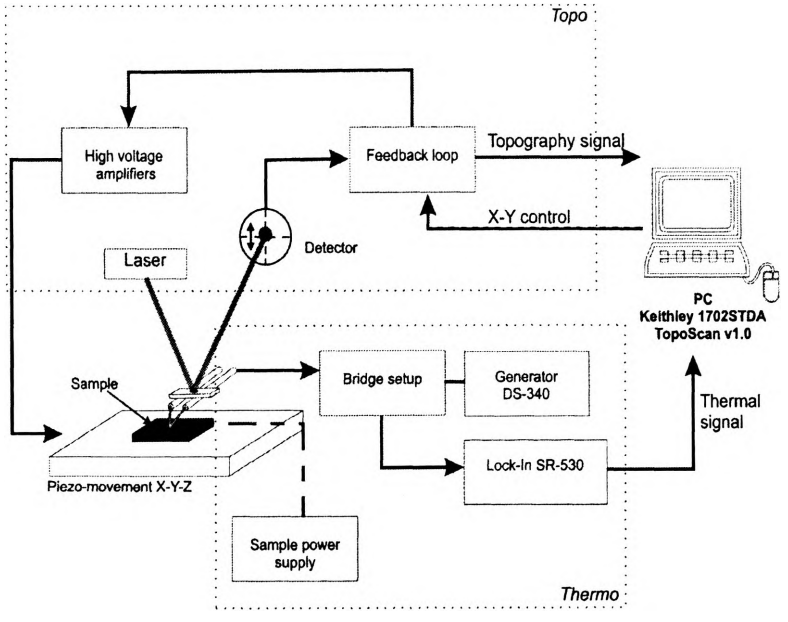

Fig. 8. Experimental setup.

This type of cantilever enables AFM-type controlling of the load force (Fig. 8). The optical signal from laser forms, after detection, input signal for electronic system and, in the next step, gives the signal proportional to the surface geometrical relief in the topographic mode.

To measure the local thermal diffusivity of a sample the thermal probe is conducted as one leg of a Wheatstone bridge. The compensation resistor in the second leg of the bridge tends to maintain balance in the circuit. When the tip of the probe is in mechanical contact with the sample, heat generated in the probe flows into the sample. The resulting change of the probe resistance gives electrical signal of unbalance of the bridge. Electrical signal from the bridge corresponds to the thermal diffusivity of the sample.

However, external feedback loop may be used for changing the voltage applied to the bridge for balancing the bridge by heating the tip of the sample. This voltage is also proportional to the thermal diffusivity of the sample.

4. Scanning thermal microscopy experiment

The AFM cantilever containing implanted resistors and metallization was used as the sample in our experiments. The piezoresistive sensor in AFM cantilever system consists of four piezoresistors in full Wheatstone bridge configuration. Two piezoresistors are placed in a longitudinal and two in a transversal direction with respect to the mechanical stress when the vertical forces act on its end (bend cantilever) Fig. 9.

During the experiment one leg of the piezoresistors bridge was powered. Thermal part of our results we present in temperature option (Fig. 10). Thermal diffusivity (conductivity) or temperature, presented as results of the experiment, depends on the action of feedback on the Wheatstone bridge (Fig. 8).

The AFM surface relief of the other part of our sample with Al metallization line deposited on the silicon dioxide is shown in Fig. 11.

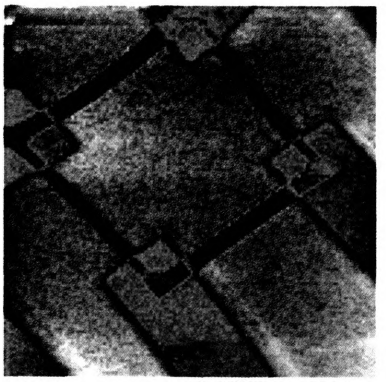

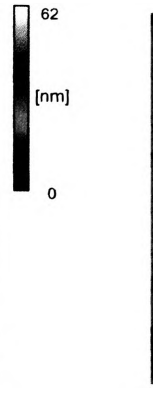

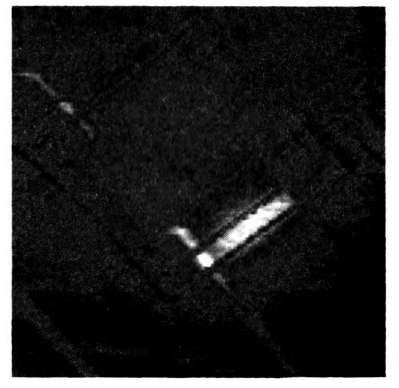

▲

Fig. 9. Piezoresistors Wheatstone bridge (scan size 75.00×75.00 μm, 128×128 lines).

Fig. 10. Thermal map of the bridge. One piezoresistor is powered.

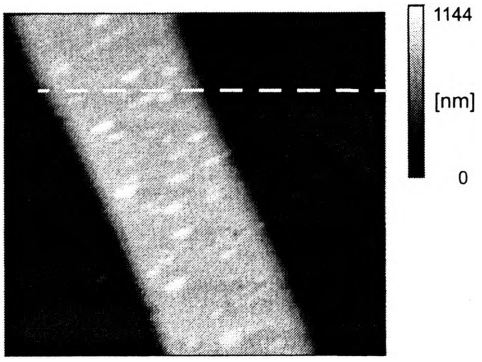

Fig. 11. AFM surface relief of Al metallization (scan size 75.00×75.00 μm, 128×128 lines). Profiles along dashed line (see Fig. 12).

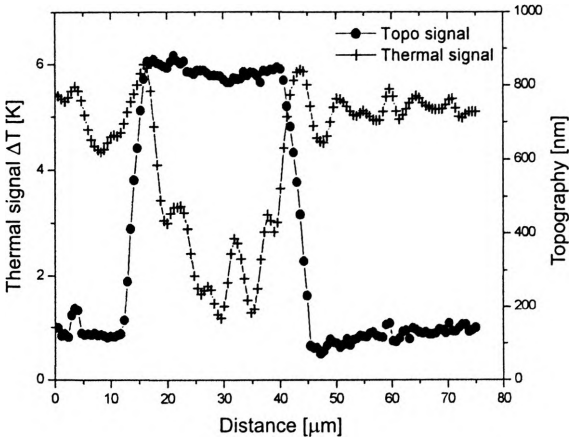

Fig. 12. AFM geometrical profile and local temperatures along the dashed line (see Fig. 11).

During this part of the experiment the sample was not powered. The SThM system acts simultaneously both in AFM and temperature contrast mode. Figure 12 shows topographical as well as thermal profiles (local thermal steady states) along dashed line.

However, each local thermal steady state is strongly linked with local thermal conductivity (diffusivity) of the sample. In this way the local temperature along the dashed line changes so much causing local differences in thermal diffusivity of silicon, silicon oxide, silicon–silicon oxide interface and thin film of aluminium.

5. Conclusions

We have presented thermal properties of two types of MEMS: the silicon cantilever (femtocalorimeter) and AFM silicon cantilever. We have used far field thermographical system with spatial resolution of the order of 10 micron as well as

SThM system. In the case of SThM, the thermal state, that is, infrared emissivity and thermal diffusivity, was determined with sub-micron spatial resolution. Additionally, the SThM system can operate simultaneously in topographical and thermal contrasts modes. Then characterization of correlations between geometrical location on the body of MEMS and its local thermal state is possible.

The SPM measuring method is relatively simple and advantages of these techniques are evident for many new applications [21]–[26].

Acknowledgments – This work was financially supported by State Committee for Scientific Research (KBN), grant No. 4T111300224.

References

[1] CHEN G., BORCA-TASCIUC T., YANG B., SONG D., LIU W.L., ZENG T., ACHIMOW D.A., Therm. Sci. Eng. 7 (1999), 43.
[2] CHEN G., Int. J. Therm. Sci. **39** (2000), 471.
[3] JOSHI A.A., MAJUMDAR A.J., Appl. Phys. **74** (1993), 31.
[4] BINNIG G., ROHRER H., Helv. Phys. Acta **55** (1982), 726.
[5] HAMMICHE A., POLLOCK H.M., SONG M., HOURSTON D.J., Meas. Sci. Technol. **7** (1996), 142.
[6] GOMES S., TRANNOY N., GROSSEL P., Meas. Sci. Technol. **10** (1999), 805.
[7] ALTES A., HEIDERHOFF R., BALK L.J., Int. J. Mod. Phys. B **16** (2002), 922.
[8] KOTCHETKOV D., ZOU J., BALANDIN A.A., Appl. Phys. Lett. **79** (2001), 4316.
[9] MILLS G., WEAVER J.M.R., HARRIS G., CHEN W., CARREJO J., JOHNSON L., ROGERS B., Ultramicroscopy **80** (1999), 7.
[10] SZELOCH R.F., GOTSZALK T.P., JANUS P., Microelectron. Reliab. **42** (2002), 1719.
[11] GOTSZALK T., GRABIEC P., RANGELOW I.W., Ultramicroscopy **82** (2000), 39.
[12] MAJUMDAR A.J., Annu. Rev. Mater. Sci. **29** (1999), 505.
[13] POLLOCK H.M., HAMMICHE A., J. Phys. D: Appl. Phys. **34** (2001), R23.
[14] PYLKKI R.J., MOYER P.J., WEST P.E., Jpn. J. Appl. Phys. **33** (1994), 3785.
[15] HAMMICHE A., HOURSTON D.J., POLLOCK H.M., READING M., SONG M., J. Vac. Sci. Technol. B **14** (1996), 1486.
[16] NAKABEPPU O., CHANDRACHOOD M., WU Y., LAI J., MAJUMDAR A., Appl. Phys. Lett. **66** (1995), 694.
[17] GOTSZALK T., GRABIEC P., HUDEK P., SHI F., BARTH W., DĘBSKI T., ZABOROWSKI M., JANUS P., RANGELOW I.W., Intern. Conf. Micro- and Nano Engineering'99 Rome, Italy, September 21–23, 1999, 257.
[18] SZELOCH R.F., GOTSZALK T.P., RADOJEWSKI J., JANUS P., ORAWSKI W., PDRAK R., Proc. MicroMat'2000, Berlin, April 17–19, 2000, 1257.
[19] SZELOCH R.F., GOTSZALK T.P., RANGELOW I., GRABIEC P., RADOJEWSKI J., JANUS P., ORAWSKI W., PDRAK R., Proc. MicroMat'2000, Berlin, April 17–19, (2000), 810.
[20] www.thermomicro.com
[21] CRAMER R.M., BRUCHHAUS L., BALK. L.J., Microelectron. Reliab. **37** (1997), 1583.
[22] MAYWALD M., PYLKKI R.J., BALK L.J., Scanning Microsc. **8** (1994), 181.
[23] HAMMICHE A., READING M., POLLOCK H.M., HOURSTON D.J., Rev. Sci. Instrum. **67** (1996), 4268.
[24] ASNIN V.M., POLLAK F.H., RAMER J., SCHURMAN M., FERGUSON I., Appl. Phys. Lett. **75** (1999), 1240.
[25] RUIZ F., SUN W.D., POLLAK F.H., VEENKATRAMAN C., Appl. Phys. Lett. **73** (1998), 1802.
[26] FLORESCU D.I., ASNIN V.M., POLLAK F.H., JONES A.M., RAMER J.C., SCHURMAN M.J., FERGUSON I., Appl. Phys. Lett. **77** (2000), 1464.

Received March 13, 2003
in revised form June 6, 2003